Journal of Sound and Vibration (2002) **257**(2), 265–282
doi:10.1006/jsvi.5057, available online at http://www.idealibrary.com on IDEAL®

VIBRATION POWER TRANSMISSION OVER A RECTANGULAR AREA OF AN INFINITE PLATE SUBJECT TO UNIFORM CONPHASE VELOCITY EXCITATION

J. DAI

Shenzhen Polytechnic, Shenzhen, People's Republic of China

AND

J. C. S. LAI

Acoustics and Vibration Unit, School of Aerospace and Mechanical Engineering, University College, The University of New South Wales, Australian Defence Force Academy, Canberra, ACT 2600, *Australia. E-mail: j.lai@adfa.edu.au*

(*Received* 26 *January* 2001, *and in final form* 30 *January* 2002)

In the study of vibration isolation, mobility is normally used to reflect the characteristics of power transmission over the contact region between the exciting machine and its supporting structure. However, recent investigations indicated that power transmission is influenced by the dimensions and shape of the contact region and the use of classical point mobility can lead to significant errors. The surface mobility of an infinite plate over a rectangular contact region subject to a uniform conphase velocity excitation has been derived using the effective point mobility concept for various aspect ratios of the contact region. Results show that power transmission is distributed in a ring-like manner, with the transmission in the central region and along the edges of the contact area being rather small. As the width-based Helmholtz number $kw/2$ increases, the ring-like region expands outward but less power is transmitted. The surface mobility decreases rapidly as Helmholtz number increases. For the same Helomholtz number, the surface mobility decreases as the aspect ratio of the contact region increases and for the same contact area, it is virtually independent of the shape of the contact region for aspect ratio less than 2 or at large Helmholtz numbers (greater than 4). Experimental measurements of a simulated infinite plate confirm the theoretical calculations. Unlike uniform conphase force excitation, the surface mobility due to uniform conphase velocity distribution does not oscillate with Helmholtz number.

1. INTRODUCTION

In the investigation of vibration isolation, the contact region between an exciting source and its supporting structure is generally simplified as a point-like connection. Cremer *et al.* [1] investigated the point mobility in infinite thin beams and infinite thin plates. However, in practical situation, the contact region between two sub-structures is finite with dimensions comparable to the governing wavelength and the excitations over the contact region may have complicated spatial distributions particularly at higher frequencies. The use of the classical point mobility estimates may result in significant errors. Thus, the vibration characteristics of a structural system and the vibration power transmission through a finite contact region have been recently explored by the concept of surface

0022-460X/02/$35.00

mobility. The vibration behaviour of infinite structures is essential for vibration power flow analysis as it has been demonstrated by Cremer *et al.* [1] that the power supplied to a finite system by a random force is equal to the power supplied by that force to a corresponding infinite system. Hence, considerable insight may be gained by studying the power flow in infinite structures.

Hammer and Petersson [2, 3] introduced the concept of strip mobility to study vibration power transmission of an infinite homogeneous thin plate excited on a strip by uniform contact force and uniform contact velocity. Subsequently, Norwood *et al.* [4] studied the surface mobility of an infinite plate over a circular contact area. By using the concept of effective point mobility introduced by Petersson and Plunt [5], Dai *et al.* [6] investigated the power transmission over a rectangular contact area of an infinite plate excited by a uniform conphase force distribution. They found that the surface mobility decreases with increasing contact area and increasing excitation frequency. The effect of the aspect ratio of the rectangular contact area on the surface mobility is significant for aspect ratios less than 5 and for Helmholtz number (based on length) greater than 2. The strip mobility is a reasonable approximation to the surface mobility over a rectangular contact area with an aspect ratio greater than 20 for Helmholtz numbers (based on length) up to 20. These theoretical results are supported by experimental measurements [7] and finite element analysis [7,8].

While a uniform force excitation applies when the isolator of the exciting machine is relatively soft compared to its supporting structure, a uniform conphase velocity excitation is realized when the isolator of the exciting machine is relatively stiff compared to its supporting structure. The objective of this study is to investigate the vibration power transmission of an infinite plate over a rectangular contact region subject to a uniform conphase velocity excitation. By using the bending wave equation and the concept of effective point mobility, the surface mobility due to uniform conphase velocity excitation is derived. The influence of the aspect ratio of a rectangular contact area is explored and compared with that of a circular contact area. The effect of the nature of excitation (i.e., uniform conphase force versus uniform conphase velocity) on the surface mobility is examined.

2. THEORETICAL CALCULATION OF THE SURFACE MOBILITY

2.1. BASIC THEORY

In the calculation of the surface mobility, only an infinite, homogeneous thin plate with no energy loss is considered. The thin plate assumption requires that the thickness of the plate is only a fraction of the governing wavelength. Thus the bending wave equation for homogeneous thin plate can be applied [1]:

$$\Delta\Delta v(x, y) - k^4 v(x, y) = \frac{\mathrm{j}\omega}{B}\sigma(x, y), \tag{1}$$

where v represents the spatial transverse velocity of the plate, k is the bending wave number, B is the flexural stiffness of the plate, $\sigma(x, y)$ is the force per unit area at point (x, y) and Δ is the two-dimensional Laplace operator. The general solution of equation (1) for an arbitrary force distribution is given in terms of the Hankel functions of the second kind as

$$v(x, y) = M_0 \iint_{S_c} \sigma(x_0, y_0)\Pi(kr)\,\mathrm{d}x_0\,\mathrm{d}y_0, \tag{2}$$

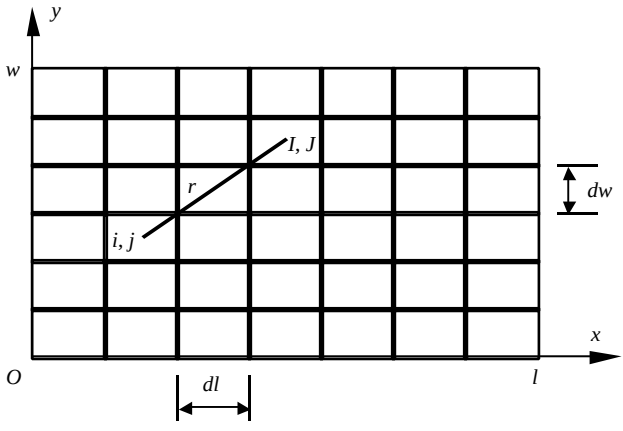

Figure 1. Discretized model of a rectangular contact area.

where $M_o = 1/(8\sqrt{B\rho})$ is the ordinary point mobility, $r = \sqrt{(x - x_o)^2 + (y - y_o)^2}$ is the distance between the excitation point (x_0, y_0) and the observation point (x, y), S_C is the excitation region, and $\Pi(kr) = \mathrm{H}_0^{(2)}(kr) - \mathrm{H}_0^{(2)}(-\mathrm{j}kr)$ is the propagation function defined as the difference between two Hankel functions of the second kind.

For a rectangular contact region firmly attached to an infinite, homogeneous thin plate, according to the boundary condition of a prescribed uniform conphase velocity distribution, equation (2) becomes an integral equation in terms of the unknown force distribution. To solve this integral equation problem, a discretized model of a contact region is used.

2.2. DISCRETIZED MODEL

A rectangular contact region can be discretized into $m \times n$ sub-regions, as shown in Figure 1 to calculate the force distribution over the contact region so that the effective point mobility and hence the surface mobility of an infinite thin plate under a uniform conphase velocity excitation can be calculated. The length and width of each sub-region are $\mathrm{d}l = l/m$ and $\mathrm{d}w = w/n$ respectively. The continuous force distribution over the contact region is approximately represented by the sum of the point forces acting at the centre of each sub-region. The point force F^{IJ} acting at the centre of sub-region (I, J) is given by

$$F^{IJ} = \int_{y_J - \mathrm{d}w/2}^{y_J + \mathrm{d}w/2} \int_{x_I - \mathrm{d}l/2}^{x_I + \mathrm{d}l/2} \sigma(x, y)\, \mathrm{d}x\, \mathrm{d}y, \tag{3}$$

where $\sigma(x, y)$ is the pressure acting over the sub-region; and (x_I, y_J) is the centre of the sub-region (I, J).

The response velocity v_{IJ}^{ij} at the centre (x_i, y_j) of the sub-region (i, j) to the force acting at (x_I, y_J) in the sub-region (I, J) can be calculated [1] as

$$v_{IJ}^{ij} = M_o F^{IJ} \Pi(kr), \tag{4}$$

where r is the distance between (x_i, y_j) and (x_I, y_J):

$$r = \sqrt{(x_I - x_i)^2 + (y_J - y_j)^2}. \tag{5}$$

Therefore, the velocity v^{ij} at (x_i, y_j) in sub-region (i, j) caused by the forces acting at the centres of all sub-regions over the contact region can be obtained as

$$v^{ij} = \sum_{I=1}^{m} \sum_{J=1}^{n} v_{IJ}^{ij} = \sum_{I=1}^{m} \sum_{J=1}^{n} M_o F^{IJ} \Pi(kr). \tag{6}$$

From equation (6), the response velocities at the centres of all sub-regions can be written as below:

$$\begin{aligned} v^{11} &= \sum_{I=1}^{m} \sum_{J=1}^{n} M_o F^{IJ} \Pi(kr), \\ v^{12} &= \sum_{I=1}^{m} \sum_{J=1}^{n} M_o F^{IJ} \Pi(kr), \\ &\vdots \\ v^{mn} &= \sum_{I=1}^{m} \sum_{J=1}^{n} M_o F^{IJ} \Pi(kr), \end{aligned} \tag{7}$$

which can be written in a matrix form of

$$\{\bar{v}\} = [T]\{\bar{F}\} \tag{8a}$$

or

$$\{\bar{F}\} = [T]^{-1}\{\bar{v}\}, \tag{8b}$$

where $\{\bar{v}\}$ consists of v^{ij}, $i = 1, \ldots, m$; $j = 1, \ldots, n$. $\{\bar{F}\}$ consists of F^{IJ}, $I = 1, \ldots, m$; $J = 1, \ldots, n$. Both $\{\bar{v}\}$ and $\{\bar{F}\}$ are column vectors with mn elements. $[T]$ is a square transfer matrix with mn rows and mn columns.

For a uniform conphase velocity excitation, the velocities over the whole contact area are constant and in phase. Without the loss of generality, a unit velocity is assumed. Hence, the velocity vector can be written as

$$\begin{aligned} \mathrm{Re}(v^{ij}) &= 1 \\ \mathrm{Im}(v^{ij}) &= 0 \end{aligned} \quad \text{for } i = 1, \ldots, m \text{ and } j = 1, \ldots, n. \tag{9}$$

By substituting the values of the velocities in equation (9) into equation (8b), the force distribution, $\{\bar{F}\}$, over the contact area can be calculated.

2.3. SURFACE MOBILITY

By using the definition of the effective point mobility [5], the effective point mobility at (x_i, y_j) in sub-region (i, j) can be expressed as

$$M^{ije} = \frac{v^{ij}}{F^{ij}}. \tag{10}$$

Since $v^{ij} = 1$, the effective point mobility for a uniform conphase velocity excitation is given as

$$M^{ije} = \frac{1}{F^{ij}}. \tag{11}$$

The total complex power over the excited contact area is [2]

$$Q = \tfrac{1}{2}|F|^2 M^S, \tag{12}$$

where F is the total force acting over the whole contact area and M^S is the surface mobility over that region.

By discretizing the contact region into $m \times n$ sub-regions, the total complex power can be expressed in terms of the forces acting at the centres in all sub-regions and the effective point mobilities at the corresponding points as

$$Q = \frac{1}{2} \sum_{i=1}^{m} \sum_{j=1}^{n} |F^{ij}|^2 M^{ije}. \tag{13}$$

From equations (12) and (13), the surface mobility of an infinite thin plate for a uniform conphase velocity distribution over a rectangular contact region can be expressed in terms of the effective point mobility as

$$M^S = \frac{1}{|F|^2} \sum_{i=1}^{m} \sum_{j=1}^{n} |F^{ij}|^2 M^{ije}. \tag{14}$$

All calculations reported here were made using MATLAB version 5·0 on a SUN SPARC 20 workstation. The spatial distribution of power transmission over a rectangular contact area subject to a uniform conphase velocity excitation was investigated using effective point mobilities for two aspect ratios, namely, $l/w = 1$ (square) and $l/w = 2$. The surface mobility for various aspect ratios, $l/w = 1$, 2, 5 and 10, was calculated for a range of Helmholtz numbers.

3. FORCE DISTRIBUTIONS

By using equations (8) and (9) with $m = n = 21$, the force distributions for both square and rectangular contact areas were calculated. Figure 2 displays the amplitude of the force distributed over a square contact area for four different values of $kw/2$: 0·5, 2·5, 5 and 10. Here $kw/2$ is refereed to as the width-based Helmholtz number. It can be seen that the forces acting along the edges of the contact area are much higher than those acting at the central region of the contact area under a uniform conphase velocity excitation. The forces at the corners of the contact area are the largest. The force distribution over the square contact area is symmetrical with respect to the x- and y-axis if the origin of the Cartesian coordinate system is translated to the centre of the contact area. Figure 3(a) displays the distribution of the amplitude of the forces along the central cross-section ($y/w = 0{\cdot}5$) of the contact area. It can be seen that the forces are very small over the central part of the contact area but very large near the edges. As $kw/2$ increases, the amplitude of the force over the central part of the contact area increases and the relative differences between the force in the central part and that near the edge decrease. Figure 3(b) displays the distribution of the phase of the forces along the central cross-section ($y/w = 0{\cdot}5$) of the contact area. It can be seen that the phase near the edge oscillates around $\pi/2$ which is the phase of the forces in the central part of the contact area. The phase of the forces rises rapidly from 0° at the edge to 180° out of phase (π) and then oscillates at about 90° out of phase ($\pi/2$). In the central part of the contact area, a steady phase difference of $\pi/2$ predominates.

For a rectangular contact area ($l/w = 2$), the calculated spatial force distributions for four different values of $kw/2 = 0{\cdot}5$, 2·5, 5 and 10 are shown in Figure 4. The distribution of the amplitude and phase of the forces along a mid-line of the contact area are shown in Figures 5 and 6 respectively. These results are similar to those from Figures 2 and 3 for

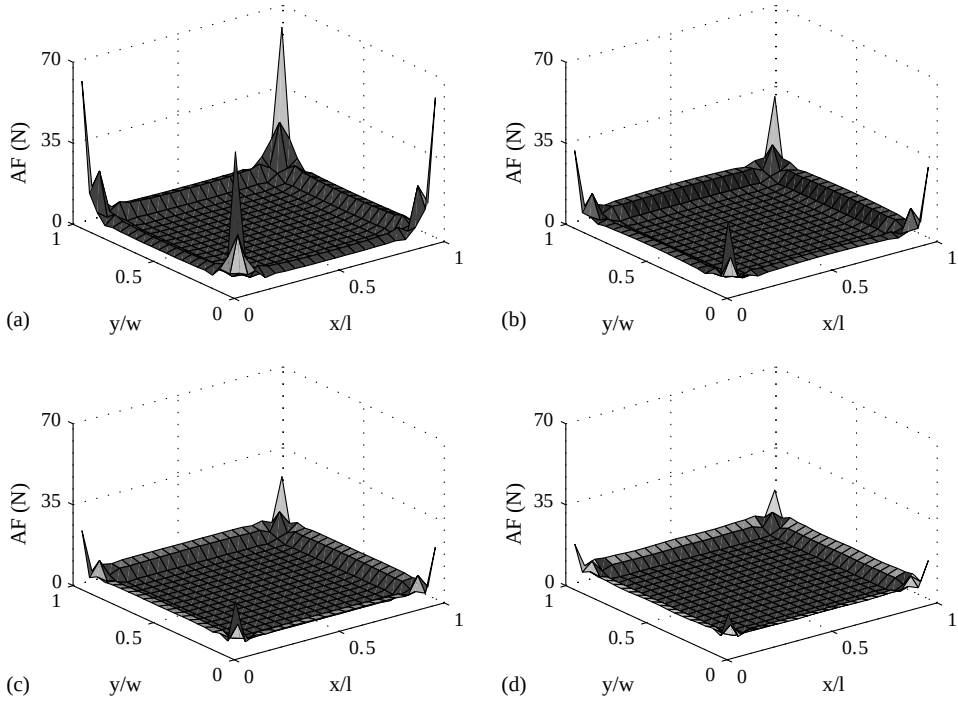

Figure 2. The spatial distribution of the amplitude of forces (AF) over a square contact area for various values of $kw/2$: (a) 0·5; (b) 2·5; (c) 5; (d) 10.

a square contact area except that the forces along the long edges are much larger than those along the short edges, due to the influence of the aspect ratio. Figures 5 and 6 are used to highlight the differences in the amplitude and phase of the forces along the x and y directions respectively. Figure 5 shows that except near the edges (i.e., $x/l \leqslant 0{\cdot}4$ or $x/l \geqslant 1{\cdot}6$, $y/w \leqslant 0{\cdot}2$ or $y/w \geqslant 0{\cdot}8$), the magnitude of the force along a mid-line of the rectangular area is almost the same in both the x and y directions for a given $kw/2$. Furthermore, in both the x and y directions, as $kw/2$ increases, the magnitude of the force increases. Figure 6 shows that, as $kw/2$ increases, the central part of the rectangular contact area where the phase is approximately $\pi/2$ increases.

4. EFFECTIVE POINT MOBILITY DISTRIBUTIONS

Since the real part of the effective point mobility reflects the amount of power transmitted into the supporting plate, it has been calculated for a square and a rectangular contact area using equation (11).

Figure 7 displays the spatial distribution of the real part of the effective point mobility over a square contact area for four values of $kw/2$ (0·5, 2·5, 5 and 10). It can be seen that the distribution over a square contact area is symmetrical about the x- and y-axis if the origin of the co-ordinate system is set at the centre of the contact area. Although the forces near the edges of the contact are very large (Figure 2), the real part of the effective point mobility here is very small. Large values of the real part of the effective point mobility, representing significant power transmission, occur nearer the central region of the contact area. As $kw/2$ increases, the main region of power transmission expands outward but the transmitted

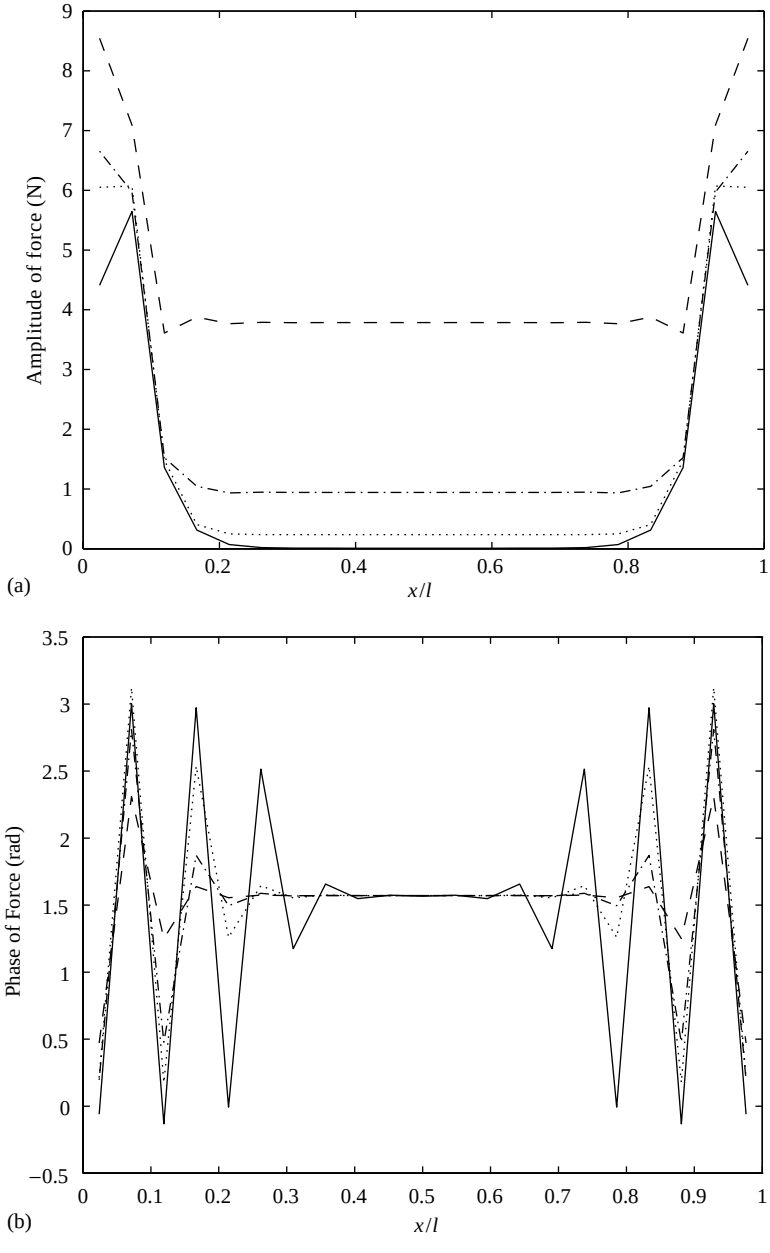

Figure 3. (a) The distribution of the amplitude of forces along the central cross-section ($y/w = 0{\cdot}5$) of a square contact area: (——) $kw/2 = 0{\cdot}5$; (·····) $kw/2 = 2{\cdot}5$; (-·-·-·-·-) $kw/2 = 5$; (---------) $kw/2 = 10$.

power becomes smaller and smaller. It can be seen from Figure 7 that the main region of power transmission over the contact area is a ring-like region which moves outward with increasing $kw/2$. Furthermore, the real part of the effective point mobility can be positive or negative, indicating that there exist some points through which the power is transmitted into the supporting plate (positive value) and other points where power is transmitted from the supporting plate back to the exciting machine (negative value). Figure 8 shows the distribution of the real part of the effective point mobility along a central cross-section in

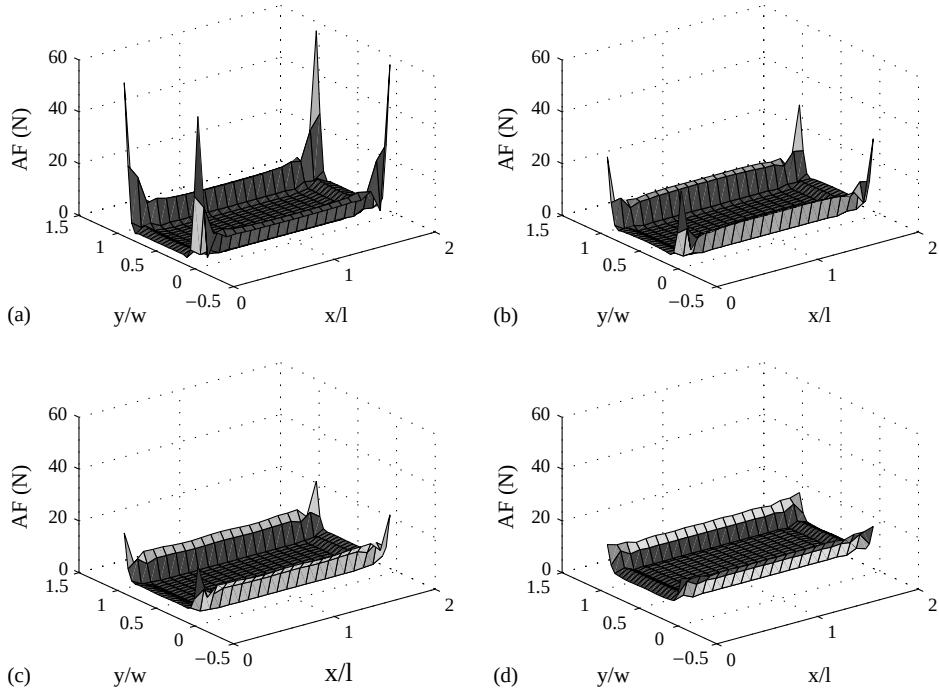

Figure 4. The spatial distribution of the amplitude of forces (AF) over a rectangular contact area with aspect ratio of 2 for various values of $kw/2$: (a) 0·5; (b) 2·5; (c) 5; (d) 10.

the x direction ($y/w = 0{\cdot}5$) for four values of $kw/2$ (0·5, 2·5, 5 and 10). It is clear that the real part of the effective point mobility decreases rapidly with increasing $kw/2$.

Figure 9 displays the spatial distribution of the real part of the effective point mobility over a rectangular contact area with an aspect ratio l/w of 2 for four values of $kw/2$ (0·5, 2·5, 5 and 10). It can be seen that the distributions of the effective point mobility are symmetrical with respect to $y/w = 0{\cdot}5$ and $x/l = 1$, but assume different values in the x and y directions. Thus, the power transmission is different in the x and y directions due to the effect of aspect ratio of the contact area. For small $kw/2$ (such as 0·5), the real part of the effective point mobility assumes very large values near the edges compared with that at the edges and in the central part of the contact area. As $kw/2$ increases, the differences in the values of the real part of the effective point mobility between different parts of the contact area reduce substantially. Figure 10 displays the distribution of the real part of the effective point mobility along the central cross-section in the x and y directions, respectively ($x/l = 1$and $y/w = 0{\cdot}5$) for four values of $kw/2$ (0·5, 2·5, 5 and 10). Similar to the case of a square contact area, Figure 10 shows that the values of the real part of the effective point mobility decrease rapidly with increasing $kw/2$, i.e., as the wavelength becomes shorter, the power transmitted into the supporting plate reduces.

5. SURFACE MOBILITY

The surface mobility of an infinite thin plate over a rectangular contact area subject to a uniform conphase velocity excitation was calculated by equation (14) and normalized by the point mobility. Figure 11 (a) displays the variation of the real part of the normalized

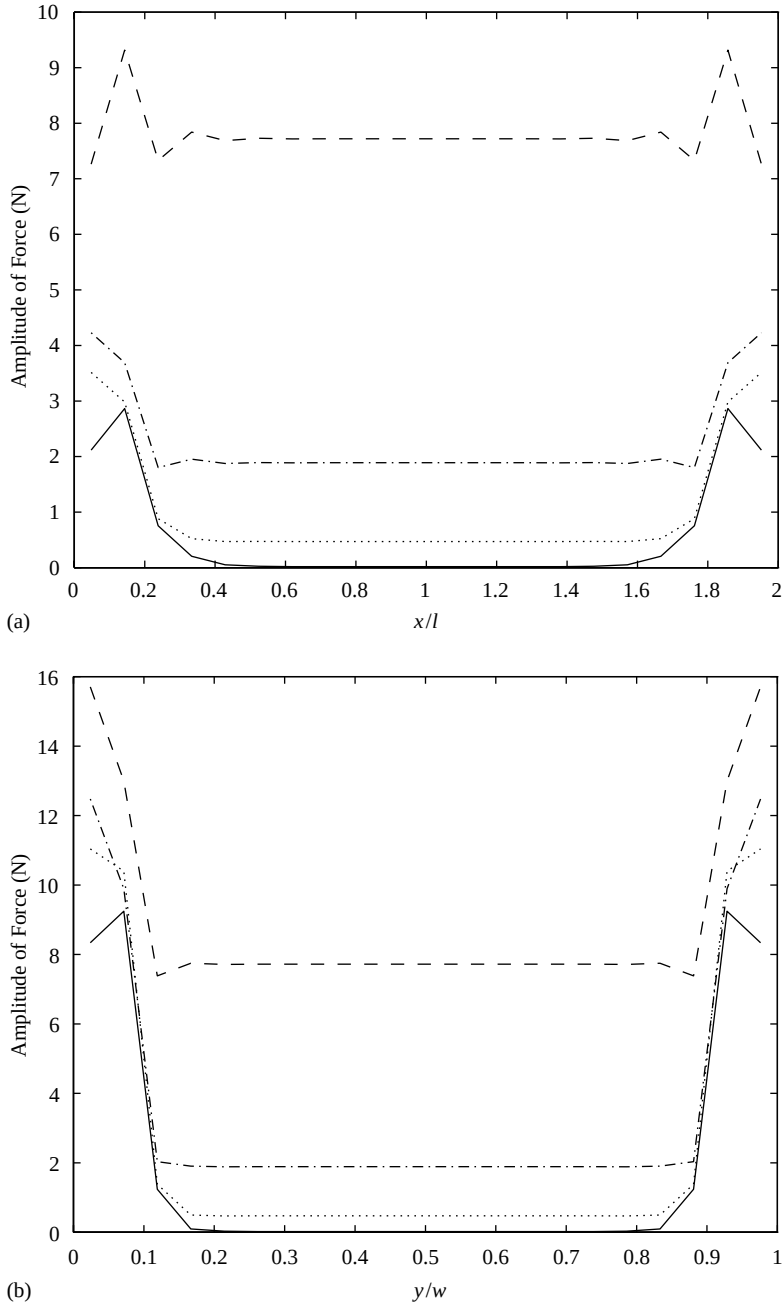

Figure 5. The amplitude of the forces along the mid-line of a rectangular contact area ($l/w = 2$): (a) in the x direction ($y/w = 0{\cdot}5$), (b) in the y direction ($x/l = 1$): (——) $kw/2 = 0{\cdot}5$; (·····) $kw/2 = 2{\cdot}5$; (-·-·-·-·-) $kw/2 = 5$; (---------) $kw/2 = 10$.

surface mobility with the Helmholtz number over a square contact area and three rectangular contact areas with an aspect ratio (l/w) of 2, 5 and 10, respectively, compared with the result for a circular contact area calculated by Norwood *et al.* [5]. It can be seen that the normalized surface mobility decreases with increasing Helmholtz number $kw/2$. As

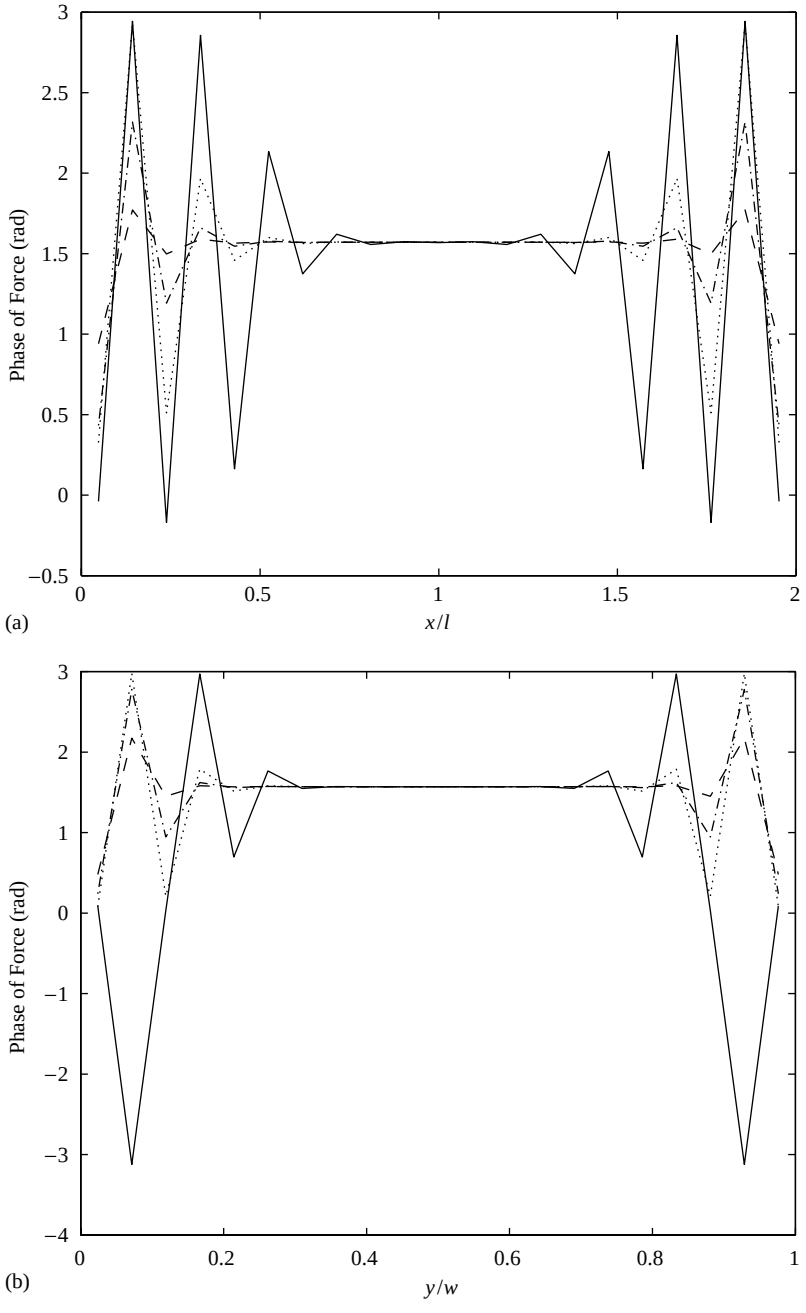

Figure 6. The phase of the forces along the mid-line of a rectangular contact area ($l/w = 2$): (a) in the x direction ($y/w = 0{\cdot}5$), (b) in the y direction ($x/l = 1$): (——) $kw/2 = 0{\cdot}5$; (·····) $kw/2 = 2{\cdot}5$; (-·-·-) $kw/2 = 5$; (- - - -) $kw/2 = 10$.

$kw/2$ increases, the power transmitted through the contact area into the supporting plate decreases markedly. Furthermore, as the aspect ratio increases, the surface mobility decreases. That is, for a given Helmholtz number, the power transmitted into the supporting plate decreases as the contact area increases.

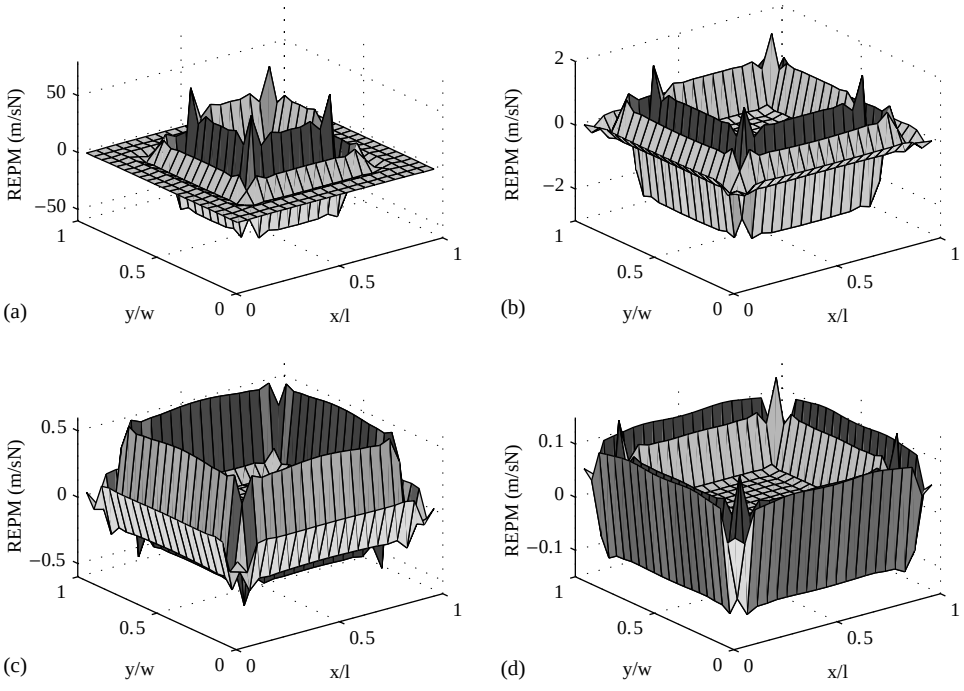

Figure 7. The real part of the effective point mobility (REPM) over a square contact area: (a) $kw/2 = 0{\cdot}5$; (b) $kw/2 = 2{\cdot}5$; (c) $kw/2 = 5$; (d) $kw/2 = 10$.

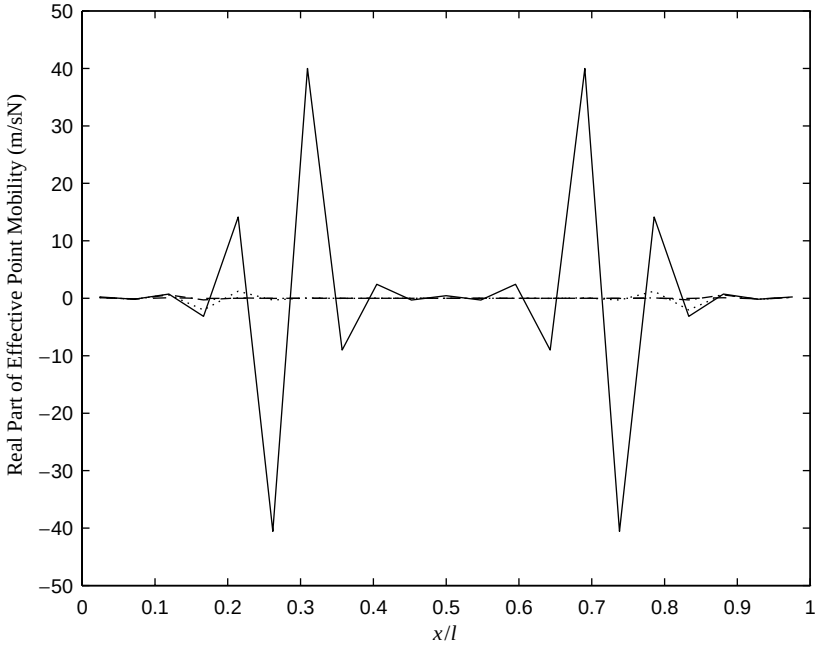

Figure 8. The real part of the effective point mobility along a central cross-section ($y/w = 0{\cdot}5$) of a square contact area: (——) $kw/2 = 0{\cdot}5$; (·····) $kw/2 = 2{\cdot}5$; (-·-·-·-) $kw/2 = 5$; (- - - - - - - - -) $kw/2 = 10$.

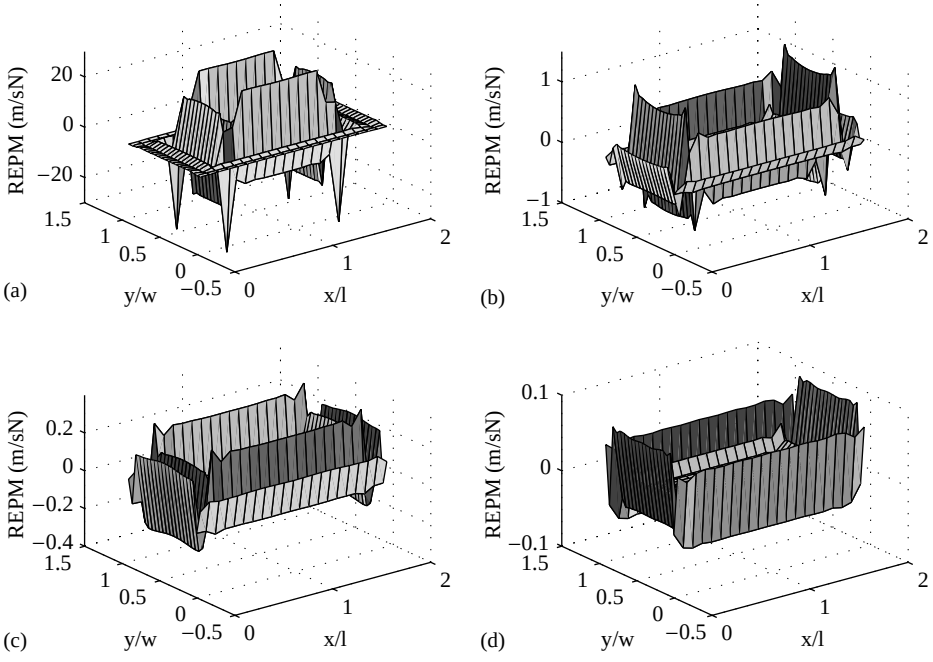

Figure 9. The real part of the effective point mobility over a rectangular contact area with an aspect ratio of 2: (a) $kw/2 = 0{\cdot}5$; (b) $kw/2 = 2{\cdot}5$; (c) $kw/2 = 5$; (d) $kw/2 = 10$.

In order to examine the effect of the shape of the contact area, the real part of the surface mobility over a square contact region, three rectangular contact regions with $l/w = 2$, 5 and 10, respectively and a circular contact region are compared in Figure 11(b) for the same contact area. Here the equivalent radius r of a rectangular contact area is defined as one which has the same circular area and is given by $w\sqrt{(l/w)/\pi}$. It can be seen from Figure 11(b) that for the same contact area, the real part of the surface mobility is almost independent of the shape of the contact region for aspect ratio l/w less than 2. In addition, it can be seen that for large Helmholtz numbers (say greater than 4), the effect of the shape of the contact area is insignificant.

The accuracy of the calculation of the surface mobility is dependent on the number of sub-regions used for the discretized model and the exciting frequency. The sensitivity of the solution to the number of sub-regions used is given in Table 1. As shown in Table 1, the surface mobility approaches the asymptotic value as the number of sub-regions increases. The result at large Helmholtz number ($kw/2 = 10$) appears to converge faster than that at small Helmholtz number ($kw/2 = 0{\cdot}5$). The relative differences between 17×17 and 21×21 sub-regions for $kw/2 = 0{\cdot}5$ and 10 are 0·95 and 0·43% respectively. Thus, for the calculations with square and rectangular contact areas presented in Figure 11, 21×21 sub-regions appear to be sufficient.

An experiment was conducted to determine the surface mobility for a uniform velocity excitation by exciting a $2{\cdot}4\ \text{m} \times 1{\cdot}2\ \text{m} \times 0{\cdot}001\ \text{m}$ aluminium plate using a rigid aluminium cone with a rectangular contact area of various aspect ratios [9]. The edges of the plate were embedded into sand so that the vibration energy transmitted in the plate was absorbed by the sand to minimize reflection. The cone was glued onto the centre of the plate and driven by a Bruel and Kjaer type 4809 shaker. Since the stiffness of the cone is much larger than that of the thin plate, it is reasonable to assume that the excitation over the contact area

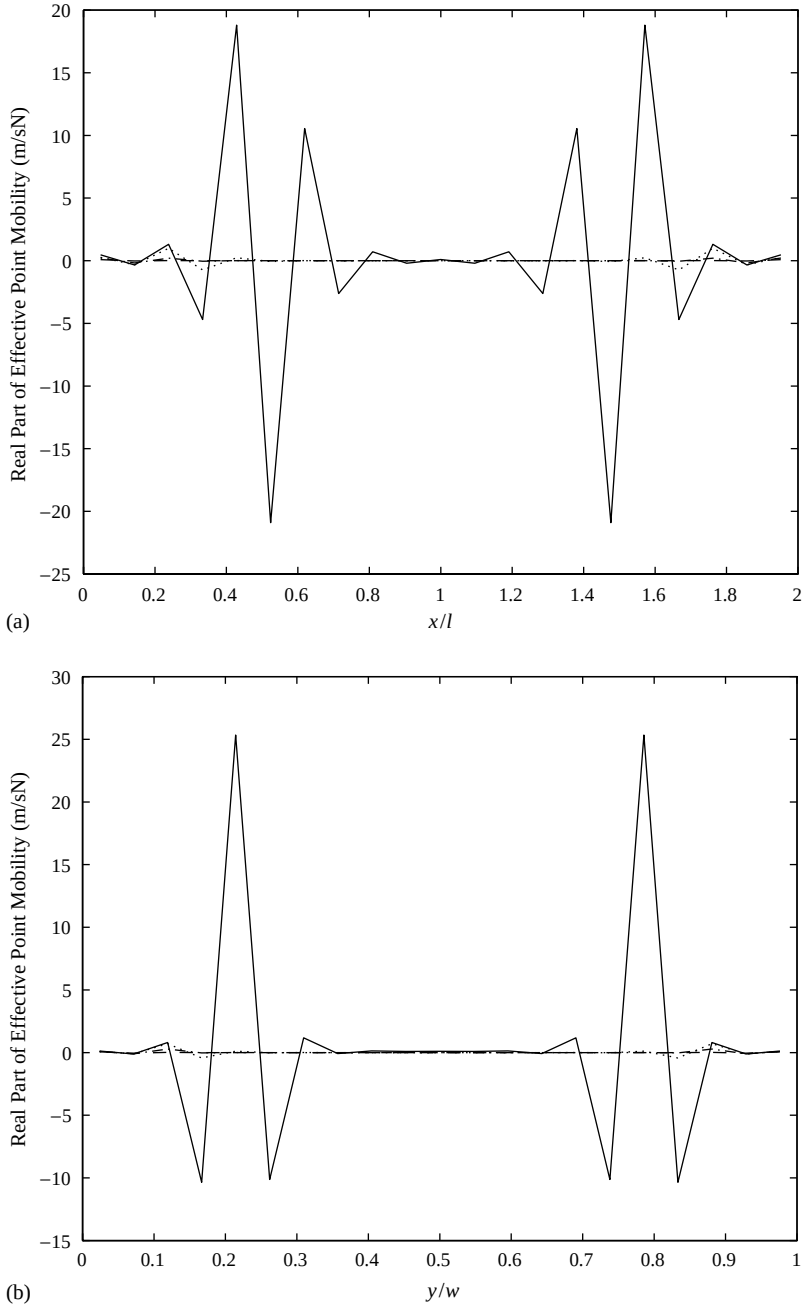

Figure 10. The real part of the effective point mobility along a mid-line of a rectangular contact area with aspect ratio of 2: (a) in the x direction ($y/w = 0{\cdot}5$), (b) in the y direction ($x/l = 1$). (——) $kw/2 = 0{\cdot}5$; (·····) $kw/2 = 2{\cdot}5$; (-·-·-) $kw/2 = 5$; (--------) $kw/2 = 10$.

approximates a uniform velocity distribution [5]. Vibration velocity measurements at three different points in the contact area indeed confirm that when the exciting frequency is greater than 250 Hz, both the amplitudes and phases at the three points are almost the same. In the experiment, the vibration velocity was measured by a B & K type 4374

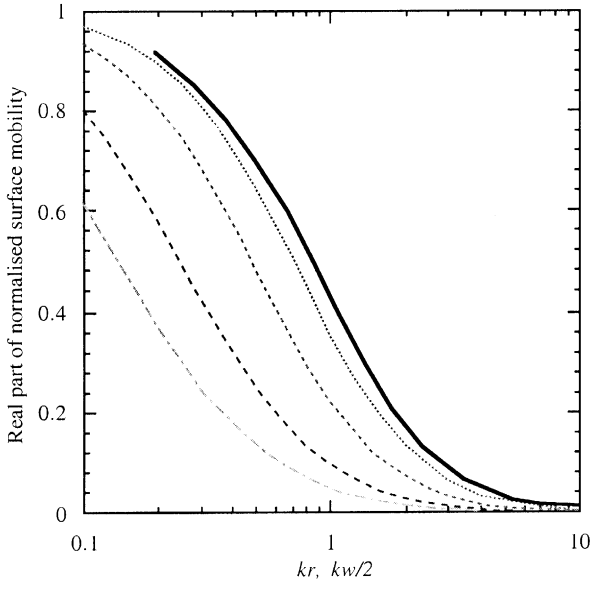

(a) same Helmholtz number

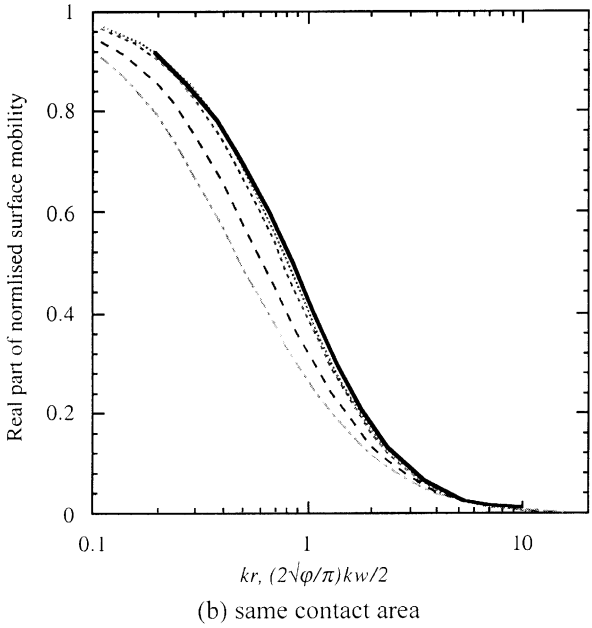

(b) same contact area

Figure 11. Surface mobility over a rectangular contact area with various aspect ratios. (——) circular; (·····) $l/w = 1$; (------) $l/w = 2$; (– – –) $l/w = 5$; (– – – –) $l/w = 10$. (a) Same Helmholtz number, (b) same contact area.

accelerometer at the centre of the contact area and the applied force was measured by a B & K type 8200 force transducer. Corrections were applied to the measurements to account for the mass loading effects due to the cone, the force transducer and the accelerometer. As shown in Figure 12(a), the real part of the normalized surface mobility over a square contact area of 75 mm × 75 mm decreases with increasing exciting frequency, in agreement with the trend predicted theoretically using equations (8), (11) and (14). For

TABLE 1

Comparison of the real parts of the normalized surface mobility over a square contact area with different number of sub-regions subject to a uniform conphase velocity excitation at $kw/2 = 0{\cdot}5$ *and* 10

	$kw/2 = 0{\cdot}5$		$kw/2 = 10$	
Sub-regions ($n \times m$)	Surface mobility	Relative differences (%)	Surface mobility	Relative differences (%)
7×7	0·6967		0·0008	
11×11	0·6683	4·25	0·0029	71·64
17×17	0·6510	2·66	0·0033	12·29
21×21	0·6449	0·95	0·0033	0·43

frequencies greater than 250 Hz, the real part of the measured surface mobility is quite smooth. However, below 250 Hz, there are quite a few peaks in the measured curve. This indicates that the assumptions of an infinite plate and a uniform conphase velocity are not valid for frequencies below 250 Hz in the experiment. Nevertheless, the agreement between the predicted and measured values is quite reasonable for frequencies greater than 250 Hz. Figure 12(b) displays both the theoretical and measured values of the real part of the normalized surface mobility over a rectangular contact area of 150 mm × 75 mm (i.e., an aspect ratio of 2). The results are very similar to those for the square contact area in Figure 12(a) but with a smaller amplitude. The agreement between the theoretical and measured values is good.

The effect of the nature of excitation on the surface mobility of an infinite plate over a rectangular area with aspect ratios $l/w = 1$ and 2 is displayed in Figures 13(a) and 13(b) for the same Helmholtz number and the same contact area respectively. Irrespective of whether the comparison is made for the same Helmholtz number or the same contact area, the real part of the normalized surface mobility decreases with increasing Helmholtz numbers for both types of excitation. However, periodic dips observed in the surface mobility due to a uniform conphase force excitation do not occur for a uniform conphase velocity excitation. Furthermore, at small Helmholtz numbers, the normalized real part of the surface mobility due to a uniform conphase force excitation is lower than that due to a uniform conphase velocity distribution but the trend is reversed at large Helmholtz numbers. These results imply that at high frequencies, vibration isolation of an infinite plate is more effective for uniform conphase force excitation than for uniform conphase velocity excitation.

6. CONCLUSIONS

The surface mobility of an infinite thin plate over a rectangular contact area subject to a uniform conphase velocity excitation has been calculated by a discretized model using the effective point mobility concept for various aspect ratios.

Results show that the forces are concentrated along the edges of the contact area. When the aspect ratio of the contact area is greater than 1, forces with large magnitude are concentrated along the long edges with compressive and tensile forces acting in different parts of the contact area. The real part of the effective point mobility, which describes the power transmission, is distributed in a ring-like manner, with its values in the central region and along the edges being rather small. It has been found that power can be transmitted

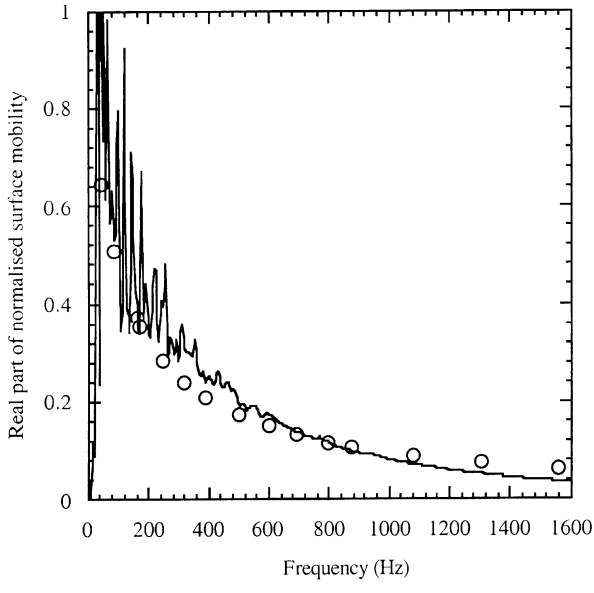

Figure 12. Comparisons of the real part of the normalized surface mobility for a rectangular contact area subject to uniform conphase velocity distribution. (a) $l/w = 1$: (○) theoretical, (——) experimental; (b) $l/w = 2$: (○) theoretical, (——) experimental.

from the exciting machine into the supporting plate or from the supporting plate back to the exciting machine. As the width-based Helmholtz number $kw/2$ increases, the ring-like region expands outward and the value of the effective point mobility decreases. The aspect ratio of the contact area also influences the distribution of the effective point mobility, leading to larger values along the long sides of the contact area.

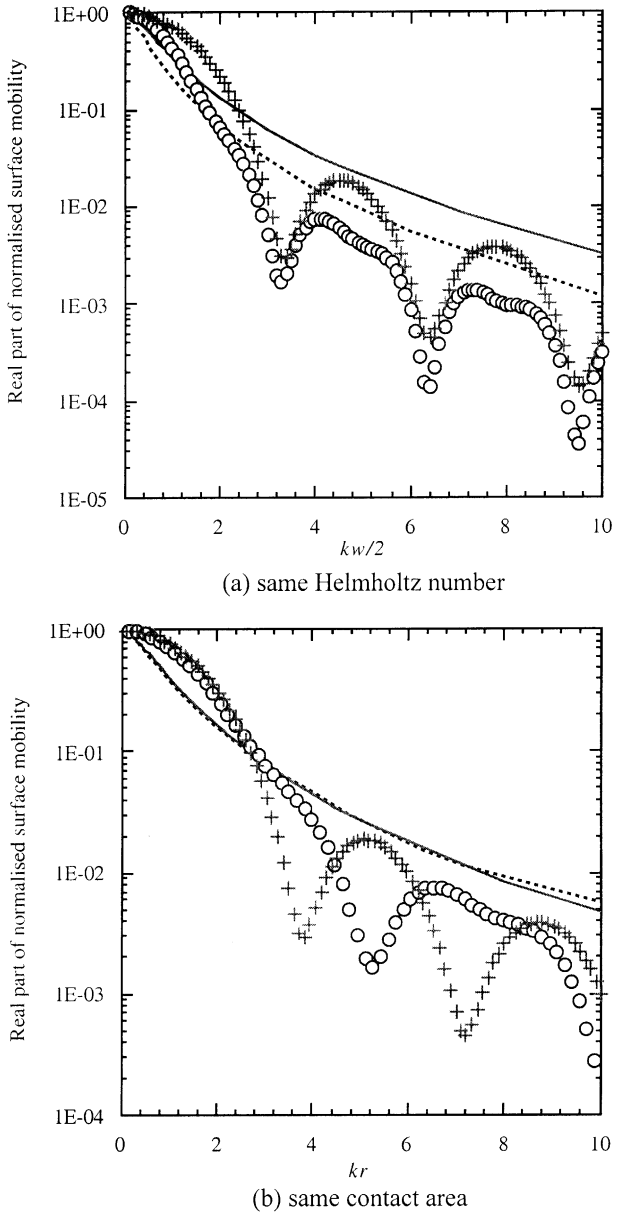

Figure 13. Comparisons of the surface mobility between uniform conphase force and uniform conphase velocity excitations. (a) Same Helmholtz number: force — (+) $l/w = 1$, (○) $l/w = 2$; velocity — (——) $l/w = 1$, (·····) $l/w = 2$. (b) Same contact area: force — (+) $l/w = 1$, (○) $l/w = 2$; velocity — (——) $l/w = 1$, (·····) $l/w = 2$.

The real part of the surface mobility decreases rapidly as width-based Helmholtz number increases. Thus the power transmitted into the supporting plate decreases with decreasing wavelength or increasing dimension of the contact region. These results agree with experimental measurements of a simulated infinite plate. Unlike the surface mobility caused by a uniform conphase force excitation, the surface mobility under uniform conphase velocity distribution does not oscillate with Helmholtz number, i.e. no dips are observed. For the same Helomholtz number, the real part of the surface mobility subject to a uniform

conphase velocity excitation decreases as the aspect ratio of the contact region increases and for the same contact area, the real part of the surface mobility is virtually independent of the shape of the contact region for aspect ratio less than 2 or at large Helmholtz numbers (greater than 4).

ACKNOWLEDGMENTS

The authors wish to express their gratitude to the Aeronautical and Maritime Research Laboratory (AMRL) of the Defence Science and Technology Organisation (DSTO) for partial support of this research. The first author (JD) acknowledges support provided by an Overseas Postgraduate Research Scholarship (OPRS) and a School of Aerospace and Mechanical Engineering Scholarship for the pursuit of this study.

REFERENCES

1. L. CREMER, M. HECKL and E. UNGAR 1988 *Strcuture-borne Sound*. Berlin: Springer-Verlag; second edition.
2. P. HAMMER and B. PETERSSON 1989 *Journal of Sound and Vibration* **129**, 119–132. Strip excitation. Part I: strip mobility.
3. P. HAMMER and B. PETERSSON 1989 *Journal of Sound and Vibration* **129**, 132–142. Strip excitation. Part 2: upper and lower bounds for the power transmission.
4. C. NORWOOD, H. M. WILLIAMSON and J. Y. ZHAO 1997 *Journal of Sound and Vibration* **202**, 95–108. Surface mobility of a circular contact area on an infinite plate.
5. B. PETERSSON and J. PLUNT 1982 *Journal of Sound and Vibration* **82**, 517–530. On the effective mobilities in the prediction of structure-borne sound transmission between a source and a receiving structure, Part 1: theoretical background and basic experimental studies.
6. J. DAI, J. C. S. LAI, H. M. WILLIAMSON and Y. J. LI 1999 *Journal of Sound and Vibration* **225**, 831–844. Investigation of vibration power transmission over a rectangular excitation area using effective point mobility.
7. J. DAI and J. C. S. LAI 2000 *Applied Acoustics* **60**, 81–93. Surface mobility over a square contact area of an infinite plate: experimental measurements and numerical prediction.
8. C. WANG and J. C. S. LAI 2000 *Journal of Sound and Vibration* **229**, 453–466. Modelling the vibration behaviour of infinite structures by FEM.
9. J. DAI and J. C. S. LAI 2001 *Applied Acoustics* **62**, 867–874. Experimental measurement of surface mobility over a rectangular contact area subject to a uniform conphase velocity excitation.